

Depressed charge gap in the triangular-lattice Mott insulator κ -(ET)₂Cu₂(CN)₃

István Kézsmárki, Y. Shimizu, G. Mihály, Y. Tokura, K. Kanoda, G. Saito

Angaben zur Veröffentlichung / Publication details:

Kézsmárki, István, Y. Shimizu, G. Mihály, Y. Tokura, K. Kanoda, and G. Saito. 2006.
"Depressed charge gap in the triangular-lattice Mott insulator κ -(ET)₂Cu₂(CN)₃." *Physical Review B* 74 (20): 201101(R). <https://doi.org/10.1103/physrevb.74.201101>.

Nutzungsbedingungen / Terms of use:

licgercopyright

Dieses Dokument wird unter folgenden Bedingungen zur Verfügung gestellt: / This document is made available under these conditions:

Deutsches Urheberrecht

Weitere Informationen finden Sie unter: / For more information see:

<https://www.uni-augsburg.de/de/organisation/bibliothek/publizieren-zitieren-archivieren/publiz/>



Depressed charge gap in the triangular-lattice Mott insulator κ -(ET)₂Cu₂(CN)₃

I. Kézsmárki,^{1,2,3} Y. Shimizu,⁴ G. Mihály,³ Y. Tokura,^{1,2,5} K. Kanoda,¹ and G. Saito⁶

¹Department of Applied Physics, University of Tokyo, Tokyo 113-8656, Japan

²Spin Superstructure Project, ERATO, Japan Science and Technology Agency (JST), Tsukuba 305-8562, Japan

³Electron Transport Research Group of the Hungarian Academy of Science and Department of Physics, Budapest University of Technology and Economics, 1111 Budapest, Hungary

⁴RIKEN, Wako, Saitama 351-0198, Japan

⁵Correlated Electron Research Center (CERC), National Institute of Advanced Industrial Science and Technology (AIST), Tsukuba 305-8562, Japan

⁶Division of Chemistry, Kyoto University, Sakyo-ku, Kyoto 606-8502, Japan

(Received 16 August 2006; published 9 November 2006)

We have investigated polarized optical conductivity for the triangular-lattice Mott insulator κ -(ET)₂Cu₂(CN)₃ over the photon-energy range of $E=8$ meV–5 eV. This compound is located far from the metal-insulator phase boundary in the bandwidth-controlled phase diagram of κ -(ET)₂X salts and consequently strong charge correlations are expected. However, its ground-state optical conductivity spectrum for polarizations within the bc plane shows no distinct charge gap in the energy range investigated, i.e., it is considerably smaller than $\Delta \approx 110$ meV, which was previously reported for the barely insulating κ -(ET)₂Cu[N(CN)₂]Cl [Kornelsen *et al.*, Solid State Commun. **81**, 343 (1992)]. We attribute the pseudo-gap-like nature of the optical spectra to strong spin fluctuations emerging in an isotropic triangular lattice. The midinfrared peak is analyzed in terms of Coulomb interaction and κ -(ET)₂Cu₂(CN)₃ is characterized by intermediate strength of electron correlation.

DOI: 10.1103/PhysRevB.74.201101

PACS number(s): 71.27.+a, 71.30.+h

Spin frustration in Mott insulator has given rich physics for the magnetic ground state of strongly interacting electrons. When Coulomb repulsion energy (U) becomes comparable to the bandwidth (W), a metal-to-insulator transition takes place as observed in a great variety of materials.¹ In the limit of strong correlations ($U \gg W$) the single band Hubbard model can be generally mapped to the Heisenberg model and the insulator phase shows inherent antiferromagnetic order. However, the role of spin degrees of freedom in the close vicinity of the Mott transition remains as an unsolved issue that is believed to be relevant to the mechanism of superconductivity appearing on the verge of the Mott boundary in the organic conductors and the high- T_c cuprates.

The family of organic molecular conductors κ -(ET)₂X [ET=bis(ethylenedithio)tetrathiafulvalene and X=monovalent anion] have provided a good arena for the study of the Mott transition in two dimensions.^{2–5} In the conducting layer, ET molecules are strongly dimerized and they form a frustrated triangular lattice.⁶ Since the valence of each ET dimer is +1, the conduction band is effectively half-filled. When the on-site Coulomb repulsion dominates over the bandwidth, the system becomes a Mott insulator above a critical ratio $(U/W)_c$.

The magnetic ground state of a Mott insulator has been known to be antiferromagnetically ordered when the triangular lattice is anisotropic, as seen in κ -(ET)₂Cu[N(CN)₂]Cl.⁷ On the other hand, effects of spin frustration are expected to emerge for a nearly isotropic triangular lattice with moderate Coulomb interaction, $U/W \gtrsim (U/W)_c$.⁸ This situation is realized in κ -(ET)₂Cu₂(CN)₃ where the unusual temperature dependence of the magnetic susceptibility and the absence of long-range magnetic order indicate a spin-liquid state in this system.⁹ By applying hydrostatic pressure or equivalently

increasing the bandwidth, these Mott insulators undergo an insulator-to-metal transition with an underlying superconducting phase.^{10,11} In this Rapid Communication we study the influence of the strong spin frustration on the low-energy excitations by optical spectroscopy.

The resistance of κ -(ET)₂Cu₂(CN)₃ is semiconductinglike in the whole temperature region. Although the large (five orders of magnitude) enhancement of $R(T)$ from room temperature down to 15 K indicates high quality of these single crystals, the Arrhenius plot in Fig. 1 does not show a simple

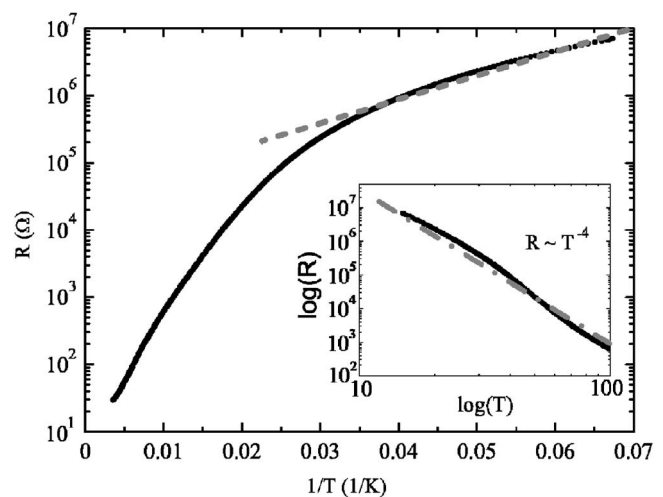


FIG. 1. Arrhenius plot of the resistance of a κ -(ET)₂Cu₂(CN)₃ single crystal. The gray dashed line at low temperature indicates the fitting of the gap value according to $R(T) = R_0 \exp(\Delta/2k_B T)$. Inset: $\log(R)$ vs $\log(T)$ plot indicative of a power-law behavior of the resistance in the low-temperature region.

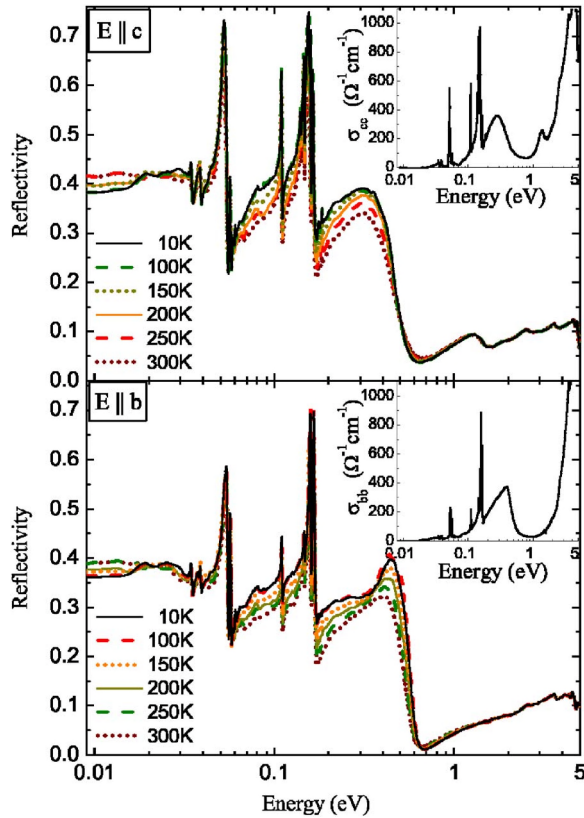


FIG. 2. (Color online) Polarized reflectivity spectra of κ -(ET) $_2$ Cu $_2$ (CN) $_3$ measured at various temperatures for $E \parallel c$ and $E \parallel b$ (upper and lower panel, respectively). The insets show the corresponding conductivity spectra at low temperature.

activated behavior as it has large curvature.

The low-temperature ($T < 30$ K) slope of the Arrhenius plot would correspond to a very small gap value, $\Delta \approx 15$ meV. A charge gap that is comparable to the exchange interaction $J \approx 20$ meV (Ref. 9) or even smaller is rather unusual in a Mott insulator. We attribute the deviation from the activated behavior to the presence of finite density of states close to the Fermi level. Indeed, the low-temperature variation of the resistivity can tentatively be described either by a $\rho \propto T^{-4}$ power-law behavior (see inset of Fig. 1) or by variable range hopping.¹² The former is indicative to a continuously diminishing density of states at the Fermi level with $D(\epsilon) \propto (\epsilon - \epsilon_F)^3$ asymptotic behavior.

To probe the finite-frequency charge dynamics in this unconventional Mott insulator, polarized reflectivity spectra of the bc plane were investigated in the photon-energy range $E = 8$ meV–5 eV below room temperature. The assignment of the distinct spectral features can be followed in Fig. 2 where the broad energy optical reflectivity and conductivity are simultaneously plotted. In agreement with former studies performed on metallic κ -(ET) $_2X$ salts^{13,14} and with first-principles band structure calculations,¹⁵ the broad conductivity peak observed above ~ 2 eV for both polarizations is ascribed to $ET^+ \rightarrow X^-$ charge-transfer excitations and to intramolecular excitations of the ET^+ molecules. At the low-energy shoulder ($E \approx 1.3$ eV) an additional peak appears only for polarization parallel to the c -axis, which was

TABLE I. Relevant energy parameters for the two κ -(ET) $_2X$ salts: t/t' describes the anisotropy of the tringular lattice and U/t is the relative strength of correlation. For details and notation see Fig. 1 of Ref. 9.

	κ -(ET) $_2$ Cu $_2$ (CN) $_3$	κ -(ET) $_2$ Cu[N(CN) $_2$] $_2$ Cl
t/t'	1.06	0.75
U/t	8.2	7.8

previously assigned to intramolecular transition of the ET^+ radical as the plane of the ET molecules is preferably oriented along the c -axis. In the following we will focus on the lower-lying ($E \lesssim 1$ eV) optical transitions.

In κ -(ET) $_2X$ salts the two-dimensional network of ET molecules is not uniform but composed of ET dimers. As the dimerization lowers the crystal symmetry, the bands arising from ET molecular orbitals split to a lower branch with bonding character and to a higher one with antibonding character. Consequently, the transition between the two branches is infrared active. The broad midinfrared (MIR) peak with maximum at $E_{dimer} \approx 0.28$ and 0.35 eV for $E \parallel c$ and $E \parallel b$, respectively, is attributed to this intradimer excitation and hereafter referred to as dimer-peak. As the clearest evidence of this assignment, this peak is observed in both κ - and β -type salts with polarization along the dimerization direction while absent in θ - and β' -type crystals where the ET molecules are stacked in a monomeric form.^{13,16} Furthermore, the location of the dimer-peak is roughly reproduced by extended Hückel tight-binding band calculations^{6,14,17} and first-principles band structure calculations.¹⁵

The analysis of the optical spectra of κ -(ET) $_2X$ salts has been so far performed on the basis of tight-binding band calculations. Tamura *et al.*¹⁴ identified the center of the dimer-peak as the intradimer transfer integral, i.e., $E_{dimer} = 2t_{b1}$. However, this approach cannot account for the magnitude of the MIR conductivity, especially in case of $E \parallel c$ when the calculated spectrum is one order of magnitude smaller than the measured one. A more fundamental issue to be considered is that κ -(ET) $_2$ Cu $_2$ (CN) $_3$ is not a simple band insulator. In fact, it is a Mott insulator at ambient pressure and the pressure-induced insulator-to-metal transition in the phase diagram of κ -(ET) $_2X$ salts is a textbook example of the bandwidth controlled Mott transition.^{9–11} As pointed out by Kino and Fukuyama,⁶ the insulator ground state cannot be reproduced by band calculations but relatively strong Coulomb interaction ($U \geq 0.76$ eV) is necessary to open a Mott gap.

In the limit of strong Coulomb interaction, the single dimer picture becomes a more appropriate starting point to describe the optical spectrum, especially in the energy range of the intradimer excitations. In this term, E_{dimer} corresponds to the effective value of the Coulomb repulsion on a dimer, $U_{eff} = [4t_{b1} + U - (U^2 + 16t_{b1}^2)^{1/2}]/2$, where t_{b1} is the intradimer transfer integral and U is the on-site Coulomb interaction on a single ET molecule.¹⁸ In the literature a consensus has been reached about the value of the intradimer transfer integral, namely $t_{b1} \approx 220$ –260 meV.^{19,22} The position of the dimer peak ($E_{dimer} \approx 280$ meV and 350 meV for $E \parallel c$ and $E \parallel b$)

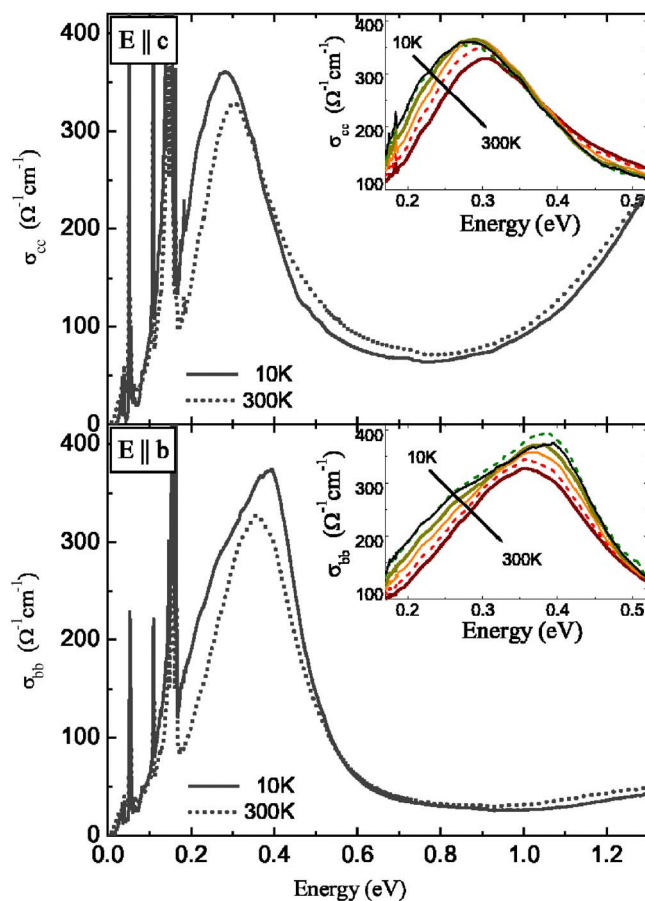


FIG. 3. (Color online) Optical conductivity spectra of $\kappa\text{-(ET)}_2\text{Cu}_2(\text{CN})_3$ at the lowest and highest temperature of the measurement for $E \parallel c$ and $E \parallel b$ shown in the upper and lower panel, respectively. The temperature evolution of the dimer peak is enlarged in the insets.

shows clear deviation from the relation $E_{\text{dimer}} = 2t_{b1}$ and suggests that Coulomb interaction must be considered. In fact, with the ratio $U/t_{b1}6$ (i.e., with $t_{b1} = 240$ meV $U = 1.5$ eV) the peak position is fairly well reproduced, as it gives $U_{\text{eff}} \approx 330$ meV. Similar ratios were deduced from spin susceptibility measurements¹⁹ and Hartree-Fock calculations⁶ (see Table I). Quantum chemistry calculations imply that for an appropriate description of $\kappa\text{-(ET)}_2X$ salts the intradimer Coulomb repulsion V (interaction between holes on neighboring molecules within the same dimer) has to be considered as well.^{20,21} With U and V of the same order of magnitude²¹ the related extended Hubbard model ($U_{\text{eff}} = \{4t_{b1} + U + V - [(U - V)^2 + 16t_{b1}^2]^{1/2}\}/2$) yields in a lower ratio, $U/t_{b1} \approx 3$. Note that the U value deduced here may be smaller than the bare on-site Coulomb energy due to the polarizability of the lattice.

On the lower edge of the dimer peak, several strong phonon modes appear for both polarizations (for a detailed analysis of the phonon modes, see, e.g., Ref. 23). The electronic part of the conductivity smoothly decreases towards zero energy without either a well-defined gap or a coherent metallic contribution. With lowering the temperature the intensity of the dimer peak is gradually increased and slightly

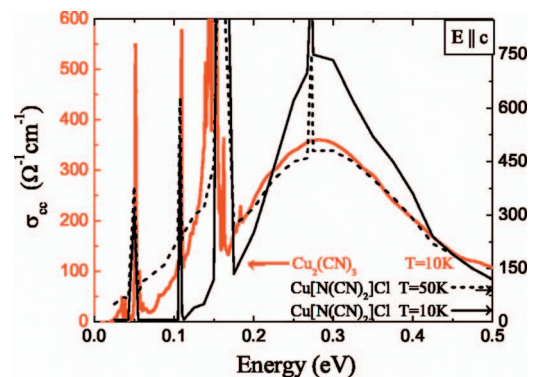


FIG. 4. (Color) Comparison of the low-temperature optical conductivity of $\kappa\text{-(ET)}_2\text{Cu}_2(\text{CN})_3$ and $\kappa\text{-(ET)}_2\text{Cu}[\text{N}(\text{CN})_2]\text{Cl}$. For the former compound, the $T = 10$ K spectrum representative for the whole $T < 100$ K range is only displayed. The conductivity spectra for $\kappa\text{-(ET)}_2\text{Cu}[\text{N}(\text{CN})_2]\text{Cl}$ are reproduced from Ref. 24. The left (right) scale corresponds to $\kappa\text{-(ET)}_2\text{Cu}_2(\text{CN})_3$ ($\kappa\text{-(ET)}_2\text{Cu}[\text{N}(\text{CN})_2]\text{Cl}$).

shifted to smaller energies. This tendency is discerned in Fig. 3 between $T = 300$ and 10 K. The detailed temperature dependence focusing on the vicinity of the dimer-peak is given in the insets, which also show that the conductivity in the far-infrared region is enhanced with lowering the temperature although it still vanishes as $\omega \rightarrow 0$. This optical weight is transferred from higher energy through an equal-absorption point at ~ 0.37 and ~ 0.55 eV in $\sigma_{cc}(\omega)$ and in $\sigma_{bb}(\omega)$, respectively.

In $\kappa\text{-(ET)}_2\text{Cu}[\text{N}(\text{CN})_2]\text{Cl}$, which has a larger bandwidth but is still located at the barely insulating side of the phase diagram, a similar spectral-weight transfer is observed below room temperature.²⁴ A comparison of the microscopic parameters for the two $\kappa\text{-(ET)}_2X$ salts is given in Table I. It is likely that temperature-induced structural changes affecting the electronic band structure or the intramolecular excitations are responsible for this tendency rather than correlation effects.

Below ~ 100 K practically no temperature dependence is found over the whole spectrum and the pseudogap-like feature of the optical conductivity seems to be persistent down to the insulating ground state. The residual conductivity below ~ 0.1 eV cannot be assigned to the multiphonon branch, while the quality of the crystals makes such a high in-gap impurity scattering unlikely.

We note that down to $T = 50$ K the same subgap tail is present in $\kappa\text{-(ET)}_2\text{Cu}[\text{N}(\text{CN})_2]\text{Cl}$.²⁴ The comparison between the low-temperature optical conductivity of the two compounds is given in Fig. 4 for polarization $E \parallel c$. In contrast to the negligible temperature dependence found in $\kappa\text{-(ET)}_2\text{Cu}_2(\text{CN})_3$ for $T \leq 100$ K, in the case of $\kappa\text{-(ET)}_2\text{Cu}[\text{N}(\text{CN})_2]\text{Cl}$ the pseudogap is turned into a real gap below ~ 50 K. The onset of the finite charge gap coincides with the enhancement of the antiferromagnetic spin correlations as reflected in the suppression of the spin susceptibility.⁹ This suggests that the charge carriers become more localized as the antiferromagnetic order develops, especially when the long-range order is established at $T_{\text{AF}} = 27$ K. On the other hand, in $\kappa\text{-(ET)}_2\text{Cu}_2(\text{CN})_3$ with almost

perfect triangular lattice the spin-liquid state extends at least down to 32 mK as no sign of antiferromagnetic order has been observed so far.⁹ We believe that the distinct difference between the low-energy charge excitations of the two compounds, i.e., the absence of clear charge gap in the ground state of $\kappa\text{-(ET)}_2\text{Cu}_2(\text{CN})_3$, is a consequence of the unquenched spin degrees of freedom in this compound. NMR spin-lattice relaxation rate measurements imply that its spin-liquid ground state has low-lying spin excitations of a gapless nature as well.⁹

Although $\kappa\text{-(ET)}_2\text{Cu}_2(\text{CN})_3$ is located far from the metal-insulator phase boundary, i.e., stronger charge correlations are expected, this compound has no distinct charge gap or at least it is considerably smaller than in the barely insulating $\kappa\text{-(ET)}_2\text{Cu}[\text{N}(\text{CN})_2]\text{Cl}$. Another consequence of the depressed charge gap is reflected in the difference between the pressure-temperature phase diagram of the two systems, namely that the critical endpoint of the first-order MI transition line is as high as ~ 40 K in $\kappa\text{-(ET)}_2\text{Cu}[\text{N}(\text{CN})_2]\text{Cl}$ (Ref. 10) while it is suppressed down to ~ 20 K in $\kappa\text{-(ET)}_2\text{Cu}_2(\text{CN})_3$ (Ref. 11). Furthermore, in the latter case the suppression of the spin entropy stabilizes the Mott insulator, while in $\kappa\text{-(ET)}_2\text{Cu}_2(\text{CN})_3$ strong spin frustration is considered to make the Mott insulator unstable.

In quasi-one-dimensional charge density wave systems a similar subgap absorption is observed that is induced by the lattice fluctuations via the strong electron-phonon coupling.

Since the characteristic frequency of the related lattice dynamics is well below the lower edge of the optical investigations, in the scattering process these one-dimensional lattice fluctuations can be modeled as static intrinsic disorder. We believe that low-frequency spin fluctuations play a similar role in $\kappa\text{-(ET)}_2\text{Cu}_2(\text{CN})_3$ and they are responsible for the subgap tail of the low-temperature optical conductivity, i.e., the gapless nature of charge excitations.

In conclusion, the ground-state charge excitation spectrum of the unconventional Mott insulator $\kappa\text{-(ET)}_2\text{Cu}_2(\text{CN})_3$ shows no distinct gap structure. We attribute the pseudogap-like nature of the optical conductivity spectra to strong spin fluctuations present down to low temperatures, i.e., the spin liquid state realized on the isotropic triangular lattice with intermediate strength of electron correlation. By the analysis of the midinfrared peak we estimate the effective Coulomb repulsion to be about one order of magnitude larger than the relevant transfer integral.

This work was supported by MEXT Grants-in-Aid for Scientific Research on Priority Areas (Contract Nos. 15073204 and 17071003), by JSPS Grants-in-Aid for Scientific Research (Contract No. 15104006), by CREST-JST, and by the Hungarian Scientific Research Funds (Contract Nos. OTKA F61413 and K62441). I.K. acknowledges support from ERATO Tokura Spin Superstructure Project and from the Bolyai János research program.

¹M. Imada, A. Fujimori, and Y. Tokura, *Rev. Mod. Phys.* **70**, 1039 (1998).

²K. Kanoda, *Physica C* **282**, 299 (1997).

³K. Kanoda, *Hyperfine Interact.* **104**, 235 (1997).

⁴K. Kanoda, *J. Phys. Soc. Jpn.* **75**, 51007 (2006).

⁵T. Sasaki, I. Ito, N. Yoneyama, N. Kobayashi, N. Hanasaki, H. Tajima, T. Ito, and Y. Iwasa, *Phys. Rev. B* **69**, 064508 (2004).

⁶H. Kino and H. Fukuyama, *J. Phys. Soc. Jpn.* **64**, 2726 (1995).

⁷K. Miyagawa, A. Kawamoto, Y. Nakazawa, and K. Kanoda, *Phys. Rev. Lett.* **75**, 1174 (1995).

⁸H. Morita, S. Watanabe, and M. Imada, *J. Phys. Soc. Jpn.* **71**, 2109 (2002).

⁹Y. Shimizu, K. Miyagawa, K. Kanoda, M. Maesato, and G. Saito, *Phys. Rev. Lett.* **91**, 107001 (2003).

¹⁰F. Kagawa, K. Miyagawa, and K. Kanoda, *Nature (London)* **463**, 534 (2005).

¹¹Y. Kurosaki, Y. Shimizu, K. Miyagawa, K. Kanoda, and G. Saito, *Phys. Rev. Lett.* **95**, 177001 (2005).

¹²A. Kawamoto, Y. Honma, and K. I. Kumagai, *Phys. Rev. B* **70**, 060510(R) (2004).

¹³H. Kuroda, K. Yakushi, H. Tajima, A. Ugawa, M. Tamura, Y. Okawa, A. Kobayashi, R. Kato, H. Kobayashi, and G. Saito, *Synth. Met.* **27**, A491 (1988).

¹⁴M. Tamura, H. Tajima, K. Yakushi, H. Kuroda, A. Kobayashi, R. Kato, and H. Kobayashi, *J. Phys. Soc. Jpn.* **60**, 3861 (1991).

¹⁵R. V. Kasowski and M-H. Whangbo, *Inorg. Chem.* **29**, 360 (1990).

¹⁶C. S. Jacobsen, D. B. Tanner, J. M. Williams, U. Geiser, and H. H. Wang, *Phys. Rev. B* **35**, 9605 (1987).

¹⁷D. Jung, M. Evian, J. J. Nova, M-H. Whangbo, M. A. Beno, A. M. Kini, A. J. Shultz, J. M. Williams, and P. J. Nigrey, *Inorg. Chem.* **28**, 4516 (1989).

¹⁸This single-dimer model gives the same asymptotic value $U_{eff} = 2t_{b1}$ as the tight-binding calculations in the limit $U \gg t_{b1}$.

¹⁹T. Komatsu, N. Matsukawa, T. Inoue, and G. Sato, *J. Phys. Soc. Jpn.* **65**, 1340 (1996).

²⁰B. J. Powell and R. H. McKenzie, *J. Phys.: Condens. Matter* **18**, R827 (2006).

²¹A. Fortunelli and A. Painelli, *Phys. Rev. B* **55**, 16088 (1997).

²²K. Oshima, T. Mori, H. Inokuchi, H. Urayama, H. Yamochi, and G. Saito, *Phys. Rev. B* **38**, 938 (1988).

²³K. Kornelsen, J. E. Eldridge, H. H. Wang, and J. M. Williams, *Phys. Rev. B* **44**, 5235 (1991).

²⁴K. Kornelsen, J. E. Eldridge, H. H. Whang, H. A. Charlier, and J. M. Williams, *Solid State Commun.* **81**, 343 (1992).